ChemPubSoc Europe

DOI: 10.1002/cmdc.201600612

CHEMMEDCHEM Communications

Analogues of Dehydroacetic Acid as Selective and Potent Agonists of an Ectopic Odorant Receptor through a Combination of Hydrophilic and Hydrophobic Interactions

Bernie Byunghoon Park[+],[a] NaHye Lee[+],[b, c] YunHye Kim,[a] YoonGyu Jae,[b, c] Seunghyun Choi,[a] NaNa Kang,[c] Yu Ri Hong,[c] Kiwon Ok,[a] Jeonghee Cho,[d] Young Ho Jeon,[a] Eun Hee Lee,[a] Youngjoo Byun,*[a] and JaeHyung Koo*[b, c]

Identification of potent agonists of odorant receptors (ORs), a major class of G protein-coupled receptors, remains challenging due to complex receptor–ligand interactions. ORs are present in both olfactory and non-chemosensory tissues, indicating roles beyond odor detection that may include modulating physiological functions in non-olfactory tissues. Selective and potent agonists specific for particular ORs can be used to investigate physiological functions of ORs in non-chemosensory tissues. In this study, we designed and synthesized novel synthetic dehydroacetic acid analogues as agonists of odorant receptor 895 (Olfr895) expressed in bladder. Among the synthesized analogues, (*E*)-3-((*E*)-1-hydroxy-3-(piperidin-1-yl)allylidene)-6-methyl-2*H*-pyran-2,4(3*H*)-dione (**10**) exhibited extremely high agonistic activity for Olfr895 in Dual-Glo luciferase reporter (EC_{50} = 9 nM), Ca^{2+} imaging, and chemotactic migration assays. Molecular docking and site-directed mutagenesis studies suggested that a combination of hydrophilic and hydrophobic interactions is central to the selective and specific binding of **10** to Olfr895. The design of agonists armed with both hydrophilic and hydrophobic portions could therefore lead to highly potent and selective ligands for ectopic ORs.

Odorant receptors (ORs), the largest family of G protein-coupled receptors (GPCRs), are responsible for recognizing molecular features of odorant molecules and translating the information to the brain.[1] In general, ORs bind to a number of odorants with a wide range of binding affinities.[2] Binding of odorants to cognate ORs causes conformational changes in olfactory-type G protein (G_{olf}), leading to the activation of downstream signaling pathways.[3] Although ORs are the largest family of GPCRs (≈50% in human and ≈70% in mouse),[4] no crystal structure of an OR has been elucidated to date.[5] Although most ORs are extensively expressed in nasal olfactory sensory neurons, where they perform appropriate physiological functions, ectopic expression of ORs in non-chemosensory tissues has been recently reported.[6] Comprehensive RNA-sequence analyses of ectopically expressed ORs have been performed on a broad panel of human tissues.[7] More recently, we and other researchers demonstrated ectopic expression of ORs in a variety of tissues including pancreas, bladder, thymus, heart, brain, skin, kidney, muscle, testis, liver, gut, eye, and thyroid.[8–23] ORs might, therefore, play physiological roles beyond odor perception in non-olfactory tissues, but their exact functions remain unknown.

Given the lack of crystal structures of membrane-bound ORs, activation mechanisms have been proposed and assessed based on molecular modelling and site-directed mutagenesis.[5,24–30] In general, hydrophobic interactions between ORs and cognate odorants are the major source of binding energy. Nevertheless, some ORs such as MOR244-3 (Olfr1509) and Olfr288 have a very narrow range of ligand specificity.[31] It is crucial to identify potent ligands that are specific for particular ORs in order to understand how they recognize and distinguish different ligands at the molecular level. Some ectopic ORs are overexpressed in the cancerous state[32–34] and have been linked to pathophysiological functions such as the growth of prostate cancer cells[35] and metastasis of gastric cancer cells.[36] Sensitive and selective potent ligands for specific ORs in non-olfactory tissues can be used as biological tool compounds to elucidate the physiological functions of ectopic ORs, or to manipulate the activity of ORs and thereby regulate pathophysiological conditions. Although a number of odorants for ORs have been reported, all are relatively weak or moderate agonists for particular ORs, with EC_{50} values in the μM range. Furthermore, odorants generally possess one or more functional groups (e.g., carboxylic acids, alcohols, amines, aldehydes, ketones, thiols, and esters) that can activate multiple ORs.[37–39] Although some odorants display specificity for particular ORs,[38–40] our knowledge of the molecular pharmacology of ec-

[a] *B. B. Park,[+] Y. Kim, S. Choi, K. Ok, Prof. Y. H. Jeon, Prof. E. H. Lee, Prof. Y. Byun*
College of Pharmacy, Korea University, Sejong, 30019 (South Korea)
E-mail: yjbyun1@korea.ac.kr

[b] *N. Lee,[+] Y. Jae, Prof. J. Koo*
Department of Brain and Cognitive Sciences, DGIST, Daegu, 42988 (South Korea)
E-mail: jkoo001@dgist.ac.kr

[c] *N. Lee,[+] Y. Jae, Dr. N. Kang, Y. R. Hong, Prof. J. Koo*
Department of New Biology, DGIST

[d] *Prof. J. Cho*
Department of NanoBio Medical Science, Dankook University, Cheonan, 31116 (South Korea)

[+] *These authors contributed equally to this work.*

Supporting information and the ORCID identification number(s) for the author(s) of this article can be found under http://dx.doi.org/10.1002/cmdc.201600612.

topic ORs remains limited due to the lack of selective and specific agonists.

In this study, odorant receptor 895 (Olfr895) was identified in bladder using Gene Atlas2 microarray data through bioinformatics evaluation as described in previous studies.[8,9] We quantitatively determined the expression levels of Olfr895 and three other ORs by PCR and qPCR in the bladder using olfactory bulb (OB) tissue as a control (Figure 1 A,B). The expression

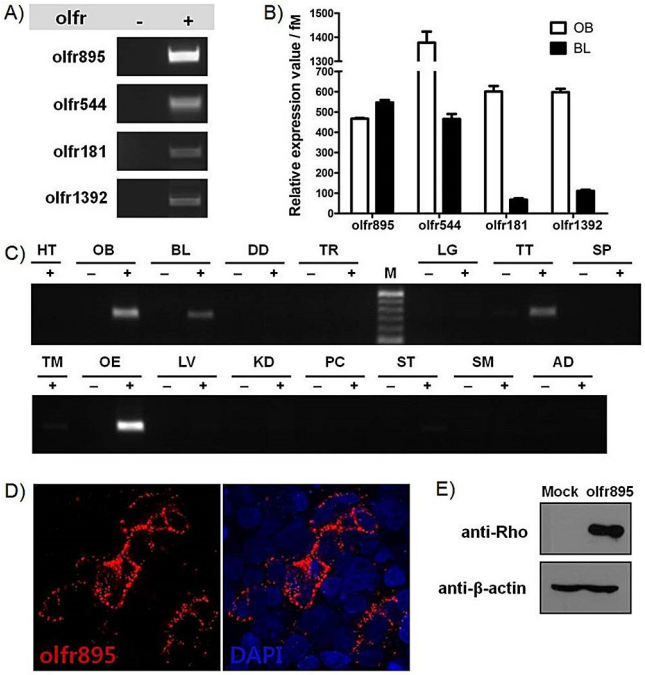

Figure 1. A) Verification of four ORs from the top-25 ORs selected by refined microarray by RT-PCR and sequencing. B) Quantification of mRNA for the four ORs by qPCR in the bladder (BL) and the olfactory bulb (OB) control olfactory tissue; values are means ± SEM. OR mRNA levels in OB and BL tissues were quantified against the Olfr544 plasmid standard and normalized against eEF-2 RNA. C) Analysis of Olfr895 expression in the OB and olfactory epithelium (OE) control tissue and in various other tissues (HT, heart; DD, duodenum; TR, thyroid; LG, lung; TT, testis; SP, spleen; TM, thymus; LV, liver; KD, kidney; PC, pancreas; ST, stomach; SM, smooth muscle; AD, adipose tissue; M, DNA ladder). D) Plasma membrane expression of Olfr895 verified using anti-rho antibody in transiently transfected HEK293 cells expressing rho-Olfr895. E) Confirmation of Olfr895 expression by western blotting with anti-rho antibody.

level of Olfr895 was higher than the other ORs in bladder tissue, and was similar to that in the OB. Next, Olfr895 expression levels in 16 tissues were determined, and the results showed that bladder is the only non-olfactory tissue expressing Olfr895, which was also expressed in the olfactory epithelium and bulb (Figure 1 C). Additionally, OR expression was observed in testis, consistent with a previous study.[6] N-terminal rho-tagged Olfr895 was cloned into a mammalian expression vector and transiently transfected with accessory proteins in HEK293 cells.[41] Non-permeable immunofluorescence staining (Figure 1 D) and western blotting (Figure 1 E) with anti-rho confirmed that the protein was localized at the plasma membrane. Anti-rho antibody was able to bind to the rho-tagged N-terminal domain of Olfr895 without membrane penetration, as ORs are typical GPCRs with seven transmembrane (TM) helices, and the N-terminus is exposed to the extracellular side of the plasma membrane. Olfr895-expressing cells exhibited a strong and non-uniform punctate expression pattern on the plasma membrane. Expression of the Olfr895 protein was clearly higher than that in controls. (Figure 1 E).

Selective and sensitive binding of the β2 adrenergic receptor (β_2AR) GPCR to ligands such as carazolol and isoproterenol proceeds via a combination of hydrophilic and hydrophobic interactions.[42] Some ORs including MOR107-1 and MOR271-1 display high selectivity in the recognition of structurally similar molecules,[37,43] implying that single OR-mediated signal transduction could be achieved by selective ligands specific for particular ORs. For instance, the human OR7D4 is selectively activated by bulky androstenones or structurally related steroids.[40] Meanwhile, mouse eugenol OR is selectively activated by bulky polycyclic compounds that bind through a combination of hydrophobic and hydrophilic interactions.[44] However, most ORs exhibit a degree of affinity for a broad spectrum for odorant ligands via weak hydrophobic interactions.[29,37] There exist very few examples of successful screening for potent and selective agonists that bind through both hydrophobic and hydrophilic interactions for targeting ectopically expressed ORs.

In this study, we designed bulky synthetic ligands specific for Olfr895 by modifying known acetyl-substituted aromatic odorants such as 2′-hydroxyacetophenone, 3′-hydroxyacetophenone, and dehydroacetic acid (Scheme 1). Commercial acetyl-substituted compounds activated Olfr895 at $>50\ \mu M$ (Table 1). To identify selective agonists of Olfr895, acetyl-substituted odorants were substituted with cyclic amines. 2′-Hydroxyacetophenone and 3′-acetophenone analogues were synthesized as described previously.[45] Preparation of compounds **9**–**13** derived from dehydroacetic acid was achieved in two steps as shown in Scheme 1. Briefly, reaction of dehydroacetic acid with *N*,*N*-dimethylformamide dimethylacetal (DMF-DMA) in xylene followed by amine exchange reaction under acidic conditions afforded enol-functionalized compounds in high yield. Enolic acid protons in **9**–**13** were observed at ≈14 ppm in ^{1}H NMR spectra.

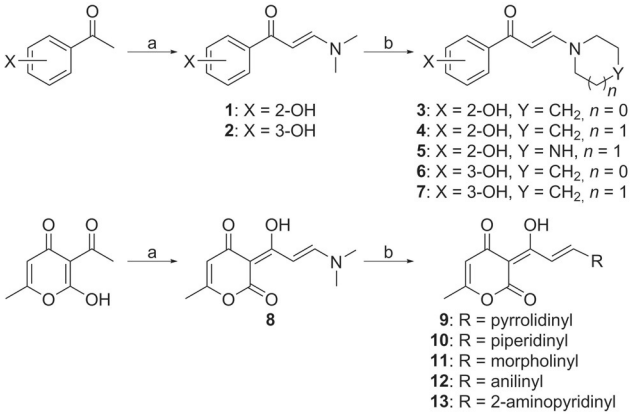

Scheme 1. Synthesis of compounds **1**–**13**. *Reagents and conditions*: a) DMF-DMA, xylene, reflux, 2 h; b) appropriate cyclic amines, acetic acid, EtOH, reflux, 2 h.

Table 1. Summary of EC_{50} values of compounds **1**–**13** and reference odorants.

Compound	EC_{50} [μM][a]
1	27.6 ± 0.05
2	3460 ± 0.21
3	54.4 ± 0.32
4	10.3 ± 0.1
5	307 ± 0.17
6	38.4 ± 0.32
7	447 ± 0.12
8	12.4 ± 0.1
9	0.091 ± 0.0007
10	0.009 ± 0.001
11	0.679 ± 0.045
12	0.386 ± 0.054
13	6.48 ± 0.05
dehydroacetic acid	258 ± 0.14
acetophenone	164 ± 0.02
2′-hydroxyacetophenone	388 ± 0.17
3′-hydroxyacetophenone	91 ± 0.2

[a] Data from luciferase activity assays were statistically analyzed using GraphPad Prism to generate EC_{50} values. Values are the mean ± SD from 3–5 independent experiments.

Activation of Olfr895 by synthesized analogues **1**–**13** was evaluated by measuring luciferase activity using Dual-Glo luciferase assays.[41] EC_{50} values of prepared compounds **1**–**13** and starting materials including 2′-hydroxyacetophenone, 3′-acetophenone and dehydroacetic acid are summarized in Table 1. Acetophenone, a broad-acting odorant activating ORs with EC_{50} values in the range of 0.1–1 mM, was used as a control.[37] Acetophenone activated Olfr895 with an EC_{50} of 164 μM, which is in the reported range.[37] Synthetic analogues **3**–**7** derived from 2′-hydroxyacetophenone or 3′-hydroxyacetophenone exhibited moderate agonistic activity for Olfr895 with EC_{50} values >1 μM. However, compounds **9**–**12** derived from dehydroacetic acid exhibited increased potency as agonists of Olfr895 with EC_{50} values <1 μM. In particular, the cyclic tertiary amine analogues **9** (pyrrolidine) and **10** (piperidine) exhibited extremely strong activation of Olfr895 with EC_{50} values of 91 nM and 9 nM, respectively. However, the morpholine-functionalized analogue **11** was less potent with an EC_{50} value of 679 nM. Introduction of aromatic amines such as aniline (**12**) and 2-aminopyridine (**13**) or acyclic tertiary dimethylamine (**8**) also decreased the agonistic activity toward Olfr895 (Table 1).

We confirmed the potency of compound **10** by measuring the activation of Olfr895 using Ca^{2+} imaging assays. We determined intracellular Ca^{2+} ($[Ca^{2+}]_i$) mobilization using Fura 2-AM ratiometric calcium imaging in Olfr895-transfected cells treated with compound **10** at various concentrations (0 nM, 1 nM, 10 nM, 1 μM, 200 μM, and 1 mM). As shown in Figure 2A, treatment of compound **10** at 1 nM and 10 nM concentrations induced the release of $[Ca^{2+}]_i$ while the control acetophenone required a much higher concentration (200 μM and 1 mM), confirming compound **10** as a strong activator of Olfr895. Next, we investigated whether compound **10** was a selective activator for Olfr895 or a broad agonist for many other ORs.

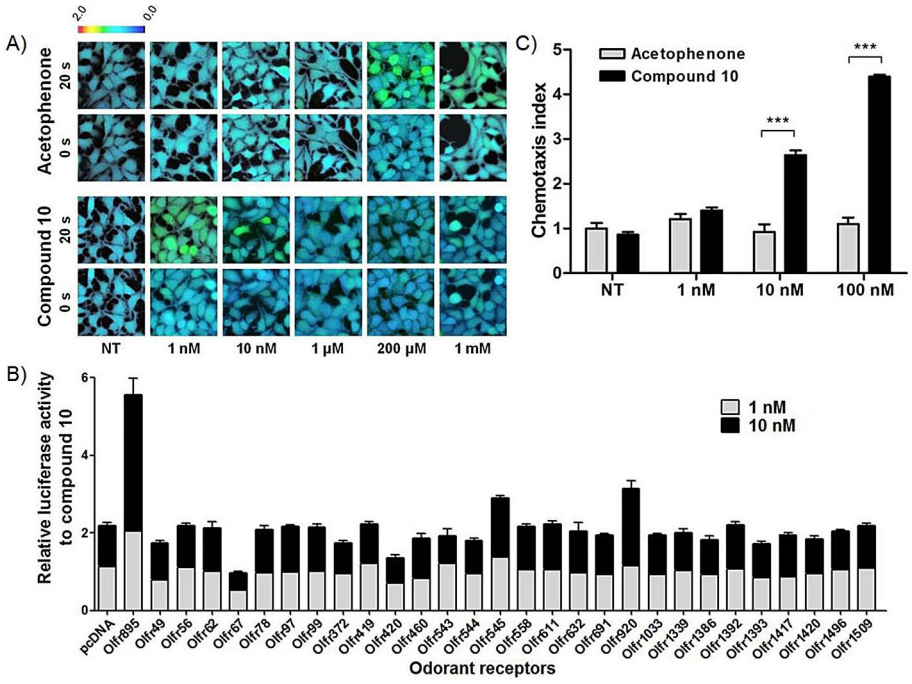

Figure 2. A) Increase in intracellular calcium in mammalian cells transfected with Olfr895 following treatment with compound **10** (bottom panel) or acetophenone (control, top panel). Images were assessed using Fura 2-AM ratiometric calcium imaging, revealing an increase in intracellular calcium mobilization after exposure to agonist for 20 s. B) Luciferase assay responses ($n=5$) of Olfr895 and 28 other ORs following incubation with compound **10**. Controls with pcDNA mock vector were included for 1 nM and 10 nM treatments. C) Stimulation of chemotactic migration by compound **10** (or acetophenone) at various concentrations (NT, 1, 10, and 100 nM) in transiently transfected mammalian cells expressing Olfr895. The migration index was determined by normalization against the total number of migrating cells in untreated controls. Data are the mean ± SEM of triplicate experiments; ***$p<0.001$ relative to acetophenone controls.

Agonistic activities for compound **10** against 29 other ORs were measured using luciferase assays, and only Olfr895 was strongly activated by compound **10,** while all other ORs were only weakly or negligibly affected (Figure 2B). Furthermore, we evaluated the effect of compound **10** on chemotactic migration of Olfr895-expressing mammalian cells. Stimulation of these cells with compound **10** resulted in high chemotactic migration (Figure 2C). At a concentration of 100 nM, compound **10** elicited a ≈4-fold increase in cell migration, and induced migration was concentration dependent (Figure 2C).

To investigate the selectivity and sensitivity of compound **10** against Olfr895, its molecular structure was determined and analyzed by single crystal X-ray diffraction and ^{1}H NMR spectroscopy. Due to the delocalization of π electrons in the conjugated enolic system, compound **10** has a planar structure with minor distortions (Figure 3A). The conjugation pattern of **10** was strikingly different from that of 2′-hydroxyacetophenone analogue **4**.[45] The carbonyl group of the conjugation system in compound **10** exists in a stable enol form (Figure 3A) rather than a keto tautomer as observed in compound **4**. This equilibrium was further corroborated by temperature-dependent ^{1}H NMR studies in diverse solvents (see Supporting Information). Strong intramolecular hydrogen bonding interactions between the enolic OH and the carbonyl oxygen of the pyrone ring were observed in the crystal structure, with an estimated bond length of 1.392 Å. The ^{1}H NMR spectrum of compound **10** also confirmed the presence of an acidic enolic OH group which appeared at 14 ppm as a broad singlet.

To investigate whether dehydroacetic acid analogues possessed strong potency against Olfr895, we performed molecular docking studies for dehydroacetic acid ligands **1**–**13** using a homology model of Olfr895 built using a high-resolution crystal structure of β1-adrenergic receptor (PDB ID: 5F8U, 3.35 Å) as a template (sequence identity = 17%, sequence similarity = 28%).[46] The ligand binding site was generated with a radius of 15 Å by selecting two key amino acids (Phe110 in TM3 and Tyr258 in TM6), which are reported to be the gate amino acids in ORs.[5] The ligands were docked in the Olfr895 homology model using the *Surflex-Dock GeomX* module (SYBYL-X 2.1.1, Tripos Inc.). The highest scoring poses of each ligand were selected and their binding modes were analyzed. Interestingly, ligands derived from dehydroacetic acid formed strong hydrogen bonding interactions with Arg171 in the active site. The stable enolic OH group of dehydroacetic acid analogues **8**–**13** also engaged in strong hydrogen bonding interactions with the guanidinium group of Arg171. In particular, compound **10** exhibited an extremely high affinity for Olfr895 due to two hydrogen bonding interactions with Arg171, with intermolecular bond distances of 1.84 and 1.93 Å, and an additional hydrogen bond with Thr198 (Figure 3B). Hydrophobic interactions between methylene groups in the cyclic ring and lipophilic amino acids (Phe110, Leu111, Val114 and Ile213) were also observed, implying that a combination of hydrophilic and hydrophobic interactions might contribute to the strong affinity of compound **10** for Olfr895. Indeed, alkylation of compounds **8** and **10** dramatically abolished the agonist activity for Olfr895 (see Supporting Information). Furthermore, replacement of the piperidine ring in **10** with a hydrophilic morpholine group resulted in a significant loss of agonistic activity. This might be due to the decreased hydrophobicity of **11**. A decrease in agonistic activity for Olfr895 was also observed for compounds **12**–**13**, even though their binding modes were similar to that of compound **10** (see Supporting Information), implying that intermolecular interactions contributed by aniline and aminopyridine moieties were less effective than those by piperidine in **10**. It has been reported that most ORs inter-

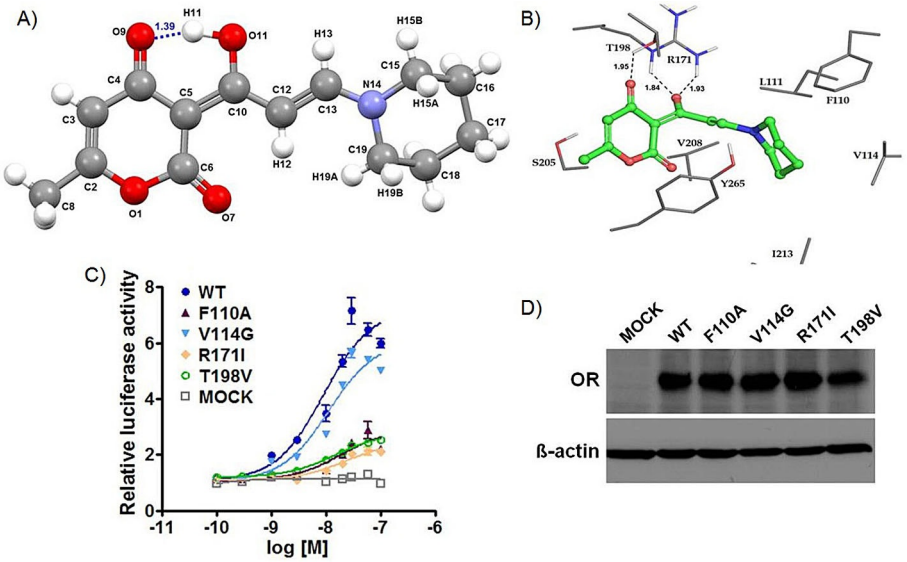

Figure 3. A) Crystal structure of compound **10**. Selected bond lengths [Å]: N(14)–C(13) 1.318 Å, N(14)–C(19) 1.467 Å, C(12)–C(13) 1.381 Å, C(10)–C(12) 1.394 Å, C(10)–O(11) 1.317 Å, C(5)–C(10) 1.453 Å, O(9)–H(11) 1.392 Å (estimated). B) Highest scoring docked pose of compound **10** in the binding cavity site of Olfr895. The dotted green lines represent hydrogen bonding interactions between **10** and Olfr895. C) EC_{50} curves for compound **10** with various Olfr895 mutants (F110A, V114G, R171I, and T198V). D) Expression of Olfr895 mutants and β-actin.

act with their corresponding odorant ligands via hydrophobic interactions, with a minimal role for hydrophilic interactions.[5,26,29,38,44,47] However, the strong binding affinity of **10** for Olfr895 could be explained by a combination of polar and nonpolar interactions, as was also observed for the binding of β_2AR agonists to β_2AR.[48]

Molecular modelling and site-directed mutagenesis experiments have been used to explore structure-function relationships of ORs with their ligands due to the lack of an available crystal structure.[5,25,26,38] Docking of compound **10** with the homology model generated in the present work indicates that the binding site is amphiphilic and consists of hydrophilic amino acid residues (Arg171 and Thr198) and hydrophobic environments (Phe110, Leu111, Val114 and Ile213) as shown in Figure 3B. When the two residues (Arg171 and Thr198) contributing to hydrophilic interactions were mutated to hydrophobic amino acids (Ile and Val), and when the hydrophobic residues (Phe110 and Val114) were replaced with non-bulky amino acids (Ala and Gly, respectively), receptor expression levels were unaffected (Figure 3D). As expected, targeted mutations R171A and T198V resulted in a significant decrease in relative luciferase activity for Olfr895 activation (by 71.5% and 67.4%, respectively) compared with wild-type Olfr895 (Figure 3C). The F110A mutation resulted in a 3-fold decrease in Olfr895 activation compared with V114G (Figure 3C). Based on molecular modelling and site-directed mutagenesis, we concluded that Arg171 and Thr198 in the loop between TM4 and TM5 are important residues for the activation of Olfr895 by compound **10**. To the best of our knowledge, this is the first report on a highly potent agonist that binds specifically to ectopic ORs via a combination of hydrophilic and hydrophobic interactions.

In conclusion, we successfully identified potent agonists of Olfr895 that is expressed in bladder, among which the piperidine-functionalized dehydroacetic acid analogue **10** strongly activated Olfr895 with an EC_{50} value of 9 nM (based on luciferase reporter, Ca^{2+} imaging, and chemotactic migration assays). This potent compound can be used as a tool compound to investigate the physiological functions of Olfr895. In addition, compound **10** may also potentially serve as a useful starting point for the development of novel antagonists of Olfr895-associated signaling pathways. Agonist-OR interactions with low affinity or specificity for particular ORs have been a bottleneck for understanding the mechanism of odor perception at the molecular level. The design of a potent and selective Olfr895 agonist by targeting both hydrophilic and hydrophobic subpockets of Olfr895 might prove useful for the identification of selective and specific agonists for other ectopic ORs.

Acknowledgements

This work was supported by the National Research Foundation of Korea (grants 2016R1A2B2009063 and 2016M3A9D5A01952414 to J.K., and grant 2014R1A4A1007304 to Y.B.), the DGIST R&D Program of the Ministry of Science, ICT & Future Planning (17-BD-06, 17-BT-02), and the Korea University Research Grant (K1504321).

Keywords: agonists · dehydroacetic acid · odorant receptors · olfr895

[1] L. Buck, R. Axel, *Cell* **1991**, *65*, 175–187.
[2] B. Malnic, J. Hirono, T. Sato, L. B. Buck, *Cell* **1999**, *96*, 713–723.
[3] D. T. Jones, R. R. Reed, *Science* **1989**, *244*, 790–795.
[4] T. K. Bjarnadóttir, D. E. Gloriam, S. H. Hellstrand, H. Kristiansson, R. Fredriksson, H. B. Schioth, *Genomics* **2006**, *88*, 263–273.
[5] C. A. de March, Y. Q. Yu, M. J. J. Ni, K. A. Adipietro, H. Matsunami, M. H. Ma, J. Golebiowski, *J. Am. Chem. Soc.* **2015**, *137*, 8611–8616.
[6] N. Kang, J. Koo, *BMB Rep.* **2012**, *45*, 612–622.
[7] C. Flegel, S. Manteniotis, S. Osthold, H. Hatt, G. Gisselmann, *PLoS One* **2013**, *8*, e55368.
[8] N. Kang, H. Kim, Y. Jae, N. Lee, C. R. Ku, F. Margolis, E. J. Lee, Y. Y. Bahk, M. S. Kim, J. Koo, *PLoS One* **2015**, *10*, e0116097.
[9] N. Kang, Y. Y. Bahk, N. Lee, Y. Jae, Y. H. Cho, C. R. Ku, Y. Byun, E. J. Lee, M. S. Kim, J. Koo, *Biochem. Biophys. Res. Commun.* **2015**, *460*, 616–621.
[10] S. H. Kim, Y. C. Yoon, A. S. Lee, N. Kang, J. Koo, M. R. Rhyu, J. H. Park, *Biochem. Biophys. Res. Commun.* **2015**, *460*, 404–408.
[11] H. Kim, N. Kang, K. W. Chon, S. Kim, N. Lee, J. Koo, M. S. Kim, *Nucleic Acids Res.* **2015**, *43*, e130.
[12] P. Garcia-Esparcia, A. Schluter, M. Carmona, J. Moreno, B. Ansoleaga, B. Torrejon-Escribano, S. Gustincich, A. Pujol, I. Ferrer, *J. Neuropathol. Exp. Neurol.* **2013**, *72*, 524–539.
[13] D. Busse, P. Kudella, N. M. Gruning, G. Gisselmann, S. Stander, T. Luger, F. Jacobsen, L. Steinstrasser, R. Paus, P. Gkogkolou, M. Bohm, H. Hatt, H. Benecke, *J. Invest. Dermatol.* **2014**, *134*, 2823–2832.
[14] A. J. Chang, F. E. Ortega, J. Riegler, D. V. Madison, M. A. Krasnow, *Nature* **2015**, *527*, 240–244.
[15] J. L. Pluznick, R. J. Protzko, H. Gevorgyan, Z. Peterlin, A. Sipos, J. Han, I. Brunet, L. X. Wan, F. Rey, T. Wang, S. J. Firestein, M. Yanagisawa, J. I. Gordon, A. Eichmann, J. Peti-Peterdi, M. J. Caplan, *Proc. Natl. Acad. Sci. USA* **2013**, *110*, 4410–4415.
[16] C. Pichavant, T. J. Burkholder, G. K. Pavlath, *Skelet Muscle* **2016**, *6*, 2.
[17] C. A. Griffin, K. A. Kafadar, G. K. Pavlath, *Dev. Cell* **2009**, *17*, 649–661.
[18] A. Grison, S. Zucchelli, A. Urzi, I. Zamparo, D. Lazarevic, G. Pascarella, P. Roncaglia, A. Giorgetti, P. Garcia-Esparcia, C. Vlachouli, R. Simone, F. Persichetti, A. R. Forrest, Y. Hayashizaki, P. Carloni, I. Ferrer, C. Lodovichi, C. Plessy, P. Carninci, S. Gustincich, *BMC Genomics* **2014**, *15*, 729.
[19] M. Spehr, G. Gisselmann, A. Poplawski, J. A. Riffell, C. H. Wetzel, R. K. Zimmer, H. Hatt, *Science* **2003**, *299*, 2054–2058.
[20] A. Pronin, K. Levay, D. Velmeshev, M. Faghihi, V. I. Shestopalov, V. Z. Slepak, *PLoS One* **2014**, *9*, e96435.
[21] C. Wu, Y. Jia, J. H. Lee, Y. Kim, S. Sekharan, V. S. Batista, S. J. Lee, *Int. J. Biochem. Cell Biol.* **2015**, *64*, 75–80.
[22] D. Priori, M. Colombo, P. Clavenzani, A. J. Jansman, J. P. Lalles, P. Trevisi, P. Bosi, *PLoS One* **2015**, *10*, e0129501.
[23] B. D. Shepard, L. Cheval, Z. Peterlin, S. Firestein, H. Koepsell, A. Doucet, J. L. Pluznick, *Sci. Rep.* **2016**, *6*, 35215.
[24] C. A. de March, S. K. Kim, S. Antonczak, W. A. Goddard, 3rd, J. Golebiowski, *Protein Sci.* **2015**, *24*, 1543–1548.
[25] S. Sekharan, M. Z. Ertem, H. Zhuang, E. Block, H. Matsunami, R. Zhang, J. N. Wei, Y. Pan, V. S. Batista, *Biophys. J.* **2014**, *107*, L5–L8.
[26] L. Gelis, S. Wolf, H. Hatt, E. M. Neuhaus, K. Gerwert, *Angew. Chem. Int. Ed.* **2012**, *51*, 1274–1278; *Angew. Chem.* **2012**, *124*, 1300–1304.
[27] L. Doszczak, P. Kraft, H. P. Weber, R. Bertermann, A. Triller, H. Hatt, R. Tacke, *Angew. Chem. Int. Ed.* **2007**, *46*, 3367–3371; *Angew. Chem.* **2007**, *119*, 3431–3436.
[28] Y. Yu, C. A. de March, M. J. Ni, K. A. Adipietro, J. Golebiowski, H. Matsunami, M. Ma, *Proc. Natl. Acad. Sci. USA* **2015**, *112*, 14966–14971.
[29] S. Katada, T. Hirokawa, Y. Oka, M. Suwa, K. Touhara, *J. Neurosci.* **2005**, *25*, 1806–1815.
[30] A. Kato, S. Katada, K. Touhara, *J. Neurochem.* **2008**, *107*, 1261–1270.
[31] X. Duan, E. Block, Z. Li, T. Connelly, J. Zhang, Z. Huang, X. Su, Y. Pan, L. Wu, Q. Chi, S. Thomas, S. Zhang, M. Ma, H. Matsunami, G. Q. Chen, H. Zhuang, *Proc. Natl. Acad. Sci. USA* **2012**, *109*, 3492–3497.
[32] L. L. Xu, B. G. Stackhouse, K. Florence, W. Zhang, N. Shanmugam, I. A. Sesterhenn, Z. Q. Zou, V. Srikantan, M. Augustus, V. Roschke, K. Carter,

D. G. McLeod, J. W. Moul, D. Soppett, S. Srivastava, *Cancer Res.* **2000**, *60*, 6568 – 6572.
[33] T. Cui, A. V. Tsolakis, S. C. Li, J. L. Cunningham, T. Lind, K. Oberg, V. Giandomenico, *Eur. J. Endocrinol.* **2013**, *168*, 253 – 261.
[34] V. Giandomenico, T. Cui, L. Grimelius, K. Oberg, G. Pelosi, A. V. Tsolakis, *J. Mol. Endocrinol.* **2013**, *51*, 277 – 286.
[35] D. Massberg, A. Simon, D. Haussinger, V. Keitel, G. Gisselmann, H. Conrad, H. Hatt, *Arch. Biochem. Biophys.* **2015**, *566*, 100 – 109.
[36] X. Guo, Z. Yang, Q. Zhi, D. Wang, L. Guo, G. Li, R. Miao, Y. Shi, Y. Kuang, *Oncotarget* **2016**, *7*, 30276 – 30294.
[37] H. Saito, Q. Y. Chi, H. Y. Zhuang, H. Matsunami, J. D. Mainland, *Sci. Signaling* **2009**, *2*, ra9.
[38] D. M. Ferrero, D. Wacker, M. A. Roque, M. W. Baldwin, R. C. Stevens, S. D. Liberles, *ACS Chem. Biol.* **2012**, *7*, 1184 – 1189.
[39] S. D. Liberles, L. B. Buck, *Nature* **2006**, *442*, 645 – 650.
[40] A. Keller, H. Y. Zhuang, Q. Y. Chi, L. B. Vosshall, H. Matsunami, *Nature* **2007**, *449*, 468 – U466.
[41] H. Zhuang, H. Matsunami, *Nat. Protoc.* **2008**, *3*, 1402 – 1413.
[42] D. M. Rosenbaum, V. Cherezov, M. A. Hanson, S. G. Rasmussen, F. S. Thian, T. S. Kobilka, H. J. Choi, X. J. Yao, W. I. Weis, R. C. Stevens, B. K. Kobilka, *Science* **2007**, *318*, 1266 – 1273.
[43] K. Yoshikawa, H. Nakagawa, N. Mori, H. Watanabe, K. Touhara, *Nat. Chem. Biol.* **2013**, *9*, 160 – 162.
[44] O. Baud, S. Etter, M. Spreafico, L. Bordoli, T. Schwede, H. Vogel, H. Pick, *Biochemistry* **2011**, *50*, 843 – 853.
[45] S. Choi, Y. Kim, B. B. Park, S. Park, J. Park, K. Ok, J. Koo, Y. W. Jung, Y. H. Jeon, E. H. Lee, K. S. Lee, Y. Byun, *J. Mol. Struct.* **2014**, *1076*, 600 – 605.
[46] A. G. Leslie, T. Warne, C. G. Tate, *Nat. Struct. Mol. Biol.* **2015**, *22*, 941 – 942.
[47] K. L. Portman, J. Long, S. Carr, L. Briand, D. J. Winzor, M. S. Searle, D. J. Scott, *Biochemistry* **2014**, *53*, 2371 – 2379.
[48] T. Warne, R. Moukhametzianov, J. G. Baker, R. Nehme, P. C. Edwards, A. G. Leslie, G. F. Schertler, C. G. Tate, *Nature* **2011**, *469*, 241 – 244.

Manuscript received: December 8, 2016
Revised: March 3, 2017
Accepted Article published: March 3, 2017
Final Article published: March 15, 2017